fibers

MDPI

Article

Effect of Temperature Exposition of Casting Solution on Properties of Polysulfone Hollow Fiber Membranes

Ilya Borisov, Vladimir Vasilevsky, Dmitry Matveev, Anna Ovcharova, Alexey Volkov and Vladimir Volkov *

A.V. Topchiev Institute of Petrochemical Synthesis, Russian Academy of Sciences, Moscow 119991, Russia; boril@ips.ac.ru (I.B.); vasilevskii@ips.ac.ru (V.V.); dmatveev@ips.ac.ru (D.M.); ovcharoff@ips.ac.ru (A.O.); avolkov@ips.ac.ru (A.V.)

* Correspondence: vvvolkov@ips.ac.ru; Tel.: +7-495-647-59-27

Received: 18 November 2019; Accepted: 11 December 2019; Published: 14 December 2019

Abstract: It was shown for the first time that the conditions of thermal treatment of the casting solution significantly affect the morphology and transport properties of porous, flat, and hollow fiber polysulfone (PSf) membranes. It is ascertained that the main solution components that are subjected to thermo-oxidative destruction are the pore-forming agent polyethylene glycol (PEG) and solvent N-methyl-2-pyrrolidone (NMP). It is proved that hydroxyl groups of PEG actively react in the process of the casting solution thermo-oxidative destruction. It is shown that despite the chemical conversion taking place in the casting solution, their stability towards coagulation virtually does not change. The differences in the membrane morphology associated with the increase of thermal treatment time at 120 °C are not connected to the thermodynamic properties of the casting solutions, but with the kinetics of the phase separation. It is revealed that the change of morphology and transport properties of membranes is connected with the increase of the casting solution viscosity. The rise of solution viscosity resulted in the slowdown of the phase separation and formation of a more densely packed membrane structure with less pronounced macropores. It is determined experimentally that with the increase of casting solution thermal treatment time, the membrane selective layer thickness increases. This leads to the decrease of gas permeance and the rise of the He/CO_2 selectivity for flat and hollow fiber membranes. In the case of hollow fibers, the fall of gas permeance is also connected with the appearance of the sponge-like layer at the outer surface of membranes. The increase of selectivity and decline of permeance indicates the reduction of selective layer pore size and its densification, which agrees well with the calculation results of the average membrane density. The results obtained are relevant to any polymeric casting solution containing NMP and/or PEG and treated at temperatures above 60 °C.

Keywords: asymmetric membranes; thermal regime; casting solution; polysulfone; flat membranes; hollow fiber membranes; morphology; transport properties

1. Introduction

Polysulfone (PSf) and polyethersulfone (PES) are among the most widely used commercial bulk polymers in the fabrication of different kinds of separation membranes [1–4]. Their good mechanical properties, high chemical resistance, and easy-to-process make these membrane materials attractive for the spinning of hollow fiber membranes suitable for a broad range of applications such as micro-, ultra-, and nanofiltration, gas separation, membrane contactors [5–8]. The general approach for the fabrication of integrally skinned asymmetric hollow fiber membranes is the

non-solvent induced phase separation (NIPS) method when the polymer is coagulated from its solution by the contact with "poor" solvent (e.g., water). The solvents traditionally used for polysulfone are N-methyl-2-pyrrolidone (NMP), dimethylformamide (DMFA), dimethylacetamide (DMAc), or dimethylsulfoxide (DMSO), which are low-volatile liquids with the boiling point above 150 °C. Meanwhile, the recent advances have been also made on the replacement of these harmful solvents by more environmentally friendly ones (methyl-5-(dimethylamino)-2-methyl-5-oxopentanoate (Rhodiasolv PolarClean®), 1,3-dimethylimidazolium dimethyl phosphate, etc.) [9–13].

The porous structure of the membrane is determined by the diffusion rate of the solvent from the casting solution into the coagulation bath and non-solvent in the opposite direction. This process is controlled by the different parameters including composition and viscosity of casting solution, the conditions of membrane fabrication (air gap height, polymers solution, and internal coagulant flow rates, etc.), the interaction between components of casting solution and coagulation bath. For instance, it was shown [14] that the presence of components (1,4-dioxane, diethylene glycol or dimethyl ether, acetone) with lower miscibility with coagulant (water) rather than solvent (NMP) resulted in a more packed and dense skin layer of the asymmetric PSf membrane; while the membrane with a more open pore structure was obtained in the case of addition of γ-butyrolactone, possessing greater miscibility with water than NMP. Higher porosity of the drainage layer and hence, permeance of resulted asymmetric membranes, can be achieved by the introduction of pore-forming components in the casting solution like polyethyleneglycol (PEG) and its derivatives [15–17], polyvinylpyrrolidone (PVP) [18–20], and surfactants [21,22].

PEG and its derivatives are more often employed as pore-forming components in the formation of asymmetric membranes. However, the casting solutions have already a high viscosity at room temperature (about 103-105 cP [17,23]), and their viscosity further increases several times with the addition of PEG [17]. To ensure the effective mixing, filtration, and degassing, the casting solution is typically prepared at an elevated temperature. Table 1 presents some examples of the protocol of preparation of casting solutions where PEG was used as the pore-forming agent. It can be noted that the casting solution was often prepared at temperature 60–130 °C in the presence of atmospheric oxygen since those polymers are thermally stable. For instance, PSf is stable for thermo-oxidative destruction for an extended period (more than a year) even at temperature 140 °C. Whereas, other components of casting solution such as NMP and PEG possess lower stability towards degradation at elevated temperatures. It was shown that NMP reacts in the presence of atmospheric oxygen at the temperature of 60–80 °C with the formation of peroxides [24], upon the destruction of which N-methylsuccinimide and atomic oxygen are formed. Thereby, NMP does not only undergo thermal degradation but can also act as a promoter of further oxidation of other components in the common solution [24]. Furthermore, PEG can also be oxidized in the presence of atmospheric oxygen forming formic acid, while PEG end groups can transform from the hydroxyl to the carbonyl, carboxyl, or ester groups [25–27]. The degradation process of PEG is associated with the reduction of its molecular weight.

Any variation in the chemical composition of the casting solution might cause certain changes in the thermodynamics and kinetics of the phase separation process during the formation of asymmetric membranes, and finally, their porous structure and separation performance. Bearing this in mind, the goal of this study was the evaluation of the influence of thermal treatment during the preparation of casting solutions on the structure and transport properties of the flat-sheet and hollow fiber membranes prepared by the non-solvent induced phase separation (NIPS) method. Polysulfone was selected as membrane material due to its good mechanical and film-forming properties, thermal and chemical stability [28]. NMP and PEG were used as a solvent and pore-forming component, respectively, due to their wide applications in the fabrication of different types of membranes.

Table 1. Conditions of fabrication of asymmetric hollow fiber membranes by non-solvent induced phase separation (NIPS) method with polyethylene glycol (PEG) as the pore-forming component.

Polymer	Pore-Forming Component	Solvent	Preparation Temperature, °C	Preparation Time, h	Ref.
PES	PEG-200, –400, –600	DMFA	80	-	[29]
PVDF	PEG-600	DMAA	60	24	[30]
PES	PEG-10000	NMP	60	48	[31]
PSf	PEG-200	NMP/water (95/5)	25–27	-	[32]
PSf	PEG-600, -6000, -20000, -35000, -150000	NMP	70	24	[33]
PES	PEG-10000	NMP	45	-	[34]
PVDF + HFP	PEG-200, -600, -6000	NMP	60	72	[35]
PSf + HBPE	PEG-400	NMP	25	24	[36]
PES	PEG-200, -600, -6000, -10000	NMP	25	-	[37]
PES	DEG	NMP	25	-	[38]
PSf	PEG-200, -400, -600, -4000, -20000, -35000	DMFA	60	12	[39]
Polylactide	PEG-6000	DMSO, NMP	130/90	3/-	[40]
PES	DEG	NMP	80	24	[41]
PSf	PEG-400	DMAA	120	4	[42]
PPSU	PEG-400, -2000, -6000, -20000, -35000, -40000	NMP	120	4	[43]

2. Experimental Part

2.1. Materials

The materials used to prepare spinning solutions were PSf pellets, Ultrason®S 6010 (from BASF, Ludwigshafen, Germany) and N-methyl-2-pyrrolidone (NMP 99% extra pure) supplied by Acros Organics, used as the base polymer and solvent, respectively, with no supplementary purification. The pore-forming additive used in the polymer solution was polyethylene glycol having an average molecular weight of 400 g/mol (PEG-400) supplied by Acros Organics (Geel, Belgium).

2.2. Preparation of Spinning Solution

For spinning solutions preparation, the mass ratio PSf to PEG-400 was 1:1.25. PSf concentration was 23.9 wt%. PSf and PEG-400 were placed into the temperature-controlled reservoir and stirred under 70 °C temperature and mixing rate 150 rpm; after that, NMP solvent was added into the solution and stirring continued under 120 °C and 500 rpm for 6–24 h. After preparation, the spinning solution was cooled to 23 ± 0.1 °C and its dynamic viscosity was measured using Brookfield viscometer DV2T-RV and RV-07 spindle (rotation speed 100 rpm). Hollow fiber membranes spinning was preceded by casting solution heating to 120 °C to reduce its viscosity. Then, the polymer solution was filtered through the metal mesh (cutoff rating 4–5 μm) under gas pressure 0.18–0.20 MPa. After filtration, the polymer solution was cooled to room temperature and degassed under vacuum.

2.3. Flat Membranes Preparation

Flat membranes were prepared according to [44]. The polymer solution was cast onto a glass plate using a casting blade; the formed thin film was subsequently immersed into distilled water. The time interval between the application of solution on the glass and immersion in water did not exceed 10 s. This time was the same for all films. The temperature of the coagulation bath (distilled water) was kept 25 °C. The resulting membranes were rinsed to remove the residual solvent and stored in

distilled water at least for 24 h. Then the membrane was sequentially washed with ethanol and hexane (each time for an hour) and dried at room temperature in air.

2.4. Fabrication of Hollow Fiber Membranes

Hollow fiber membranes were prepared via a dry–wet phase inversion technique in the free fall spinning mode in the air when bore fluid was brought into liquid polymer solution orifice, resulting in the selective layer appearance on the fibers lumen side. The air gap height was 0.8 m, the pressure above the polymer solution was 200 kPa, and the pressure above the internal coagulant was 40 kPa. After passing the air gap, the spun fiber gets into the take-up bath with water by gravity and coils of its own accord. The spinneret ring sectional area was 1.77 mm^2. Hollow fibers prepared upon contact with an aqueous medium (internal non-solvent and take-up bath with water) were subsequently treated and dried to remove residual water from pore volume. For this purpose, membranes were washed in a polar solvent (ethanol), then in nonpolar solvent (hexane) and, finally, dried under ambient conditions. The method was used to prevent capillary mesopores contraction [45], which may be present when water is drastically removed by conventional drying.

2.5. Gas Permeance Measurements

Helium and carbon dioxide were used as test gases, as their molecular mass difference provides a reliable way to determine Knudsen gas flow using the ideal selectivity value (permeability coefficients of individual gases ratio). The pure gas permeances through flat and hollow fiber membranes were measured using a volumetric membrane apparatus. The hollow fiber membrane was set inside the measuring cell. The gas flow was introduced to the internal volume of the sample. The volumetric gas flow passing through the membrane was measured using a dry gas meter (SHINAGAWA, Japan). Gas permeance measurements were carried out at room temperature (23 ± 2 °C) under transmembrane pressure from 0.5 to 2 bar while permeate gas pressure was kept constant at 1 bar. Gas permeance was calculated using the equation:

$$\frac{P}{l} = \frac{Q}{p \cdot S}\left[\frac{\mathrm{m}^3}{\mathrm{m}^2 \cdot \mathrm{h} \cdot \mathrm{atm}}\right], \quad (1)$$

where Q—gas volumetric flow rate through the membrane, m^3/h; p—transmembrane pressure, atm; S—membrane surface, m^2. The gas volumetric flow rate was calculated using the equation:

$$Q = \frac{V}{\tau}\left[\frac{\mathrm{m}^3}{\mathrm{h}}\right], \quad (2)$$

where V—the volume of gas passed through the membrane, m^3; τ—time for the specified gas volume transfer, h. The membrane area was calculated using the equation:

$$S = \pi \cdot d \cdot l\left[\mathrm{m}^2\right], \quad (3)$$

where π—constant equal to 3.14; d—hollow fiber internal diameter, m; l—fiber length, m. Ideal selectivity was calculated using the equation:

$$\alpha = \frac{(P_1/l)}{(P_2/l)} = \frac{P_1}{P_2}, \quad (4)$$

where (P_1/l)—He permeance, $m^3/(m^2 \cdot h \cdot atm)$; (P_2/l)—CO_2 permeance, $m^3/(m^2 \cdot h \cdot atm)$.

2.6. Spectrophotometric Analysis

The optical properties of casting solutions studied in this work were examined by using the spectrophotometer PE-5400UF («Ekroshim» Co. Ltd., Kaliningrad, Russia). Measurements were conducted in the regime of optical density (A) detection. The optical spectrum of the initial NMP

and NMP/PEG mixture were determined with respect to air. The change in optical density of PEG, PEG/NMP mixture, and NMP mixtures with ethylene glycol (EG) and tetraethylene glycol dimethyl ether (tetraglyme) after the thermal treatment was characterized with respect to the initial substances (untreated thermally).

2.7. Coagulation Value

The coagulation value was used as a measure of the casting solution thermodynamic stability [16]. It is equal to the weight of the H_2O/NMP mixture, added to 1 g of the casting solution at the temperature of 25 °C, when the coagulation was observed visually, and the solution does not become homogeneous in 24 h. The H_2O/NMP ratio in the coagulant was 25/75 wt%, respectively.

2.8. Scanning Electron Microscopy

Cross-sections of the hollow fiber membranes were analyzed by scanning electron microscopy (SEM) on a Hitachi Table top Microscope TM 3030 Plus with proprietary highly sensitive low-vacuum secondary electron detector (Hitachi High Technologies America Inc., Greenville, SC, USA), accelerating voltage was equal to 15 kV.

3. Results and Discussion

3.1. Effect of Heat Treatment on Spinning Solution Properties

As discussed above, the spinning solutions are typically viscous due to the high concentration of polymer and the presence of different additives such as pore-forming components (e.g., PEG). However, the defect-free hollow fibers with the desired, reproducible parameters can be yielded in the case of good homogeneity of the casting solution that makes important appropriate processing of all prior steps, including mixing, filtering, and degassing. To overcome the problem of high viscosity and to reduce the time, the spinning solution is usually processed at elevated temperatures, and in this study, the temperature of 120 °C was selected to conform to the maximal temperature used in literature to prepare casting solutions with PEG and NMP. The exposure time of PSf-based spinning solution at 120 °C was 1, 2, 6, 11, 16, and 24 h, respectively. Figure 1 shows the spinning solutions after 6, 16, and 24 h of stirring at 120 °C and 9 h at 140 °C. It can be seen that the color of the polymer solution changed from light yellow to brown with respect to exposure time and temperature, and the more intense color was found in the case of 140 °C. Figure 2 shows the optical spectra of PEG, exposed to air at 120 °C for 2, 6, and 16 h, obtained with respect to initial PEG. All spectra have a maximum of absorption at the wavelength of 250 nm, which conforms to the UV region. Since no maximums of absorbance were observed in the visible region, it can be concluded from the literature [25–27] that PEG and its degradation products are not the cause of the change of the polymer solution color. On the other hand, the increase of absorption in the UV-range with longer exposure time at 120 °C can be attributed to the degradation of PEG molecules.

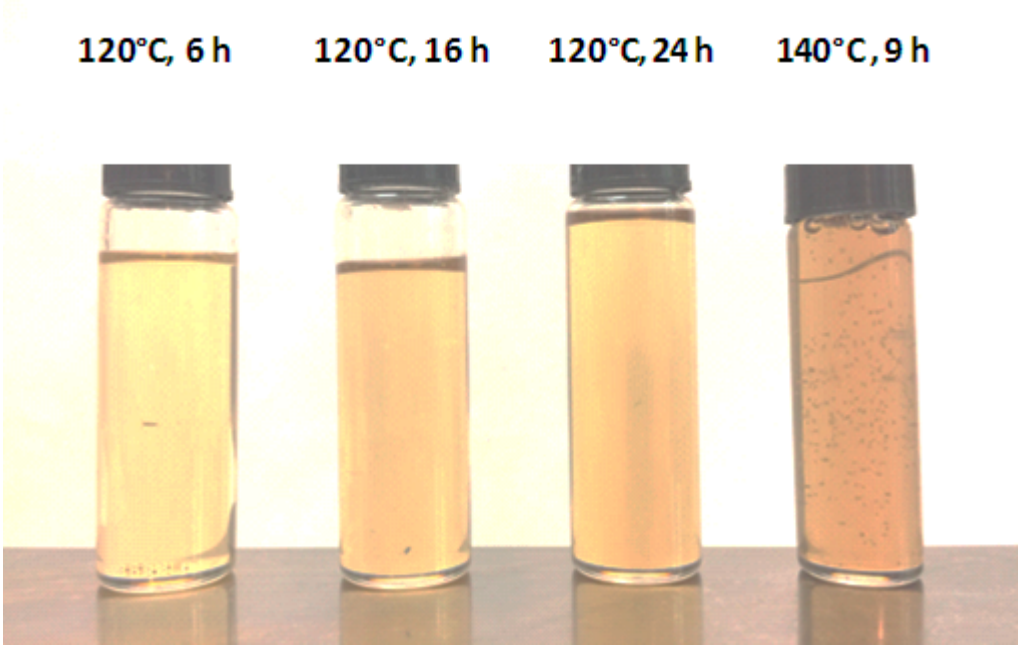

Figure 1. Photographs of casting solutions obtained at different times and temperatures of mixing.

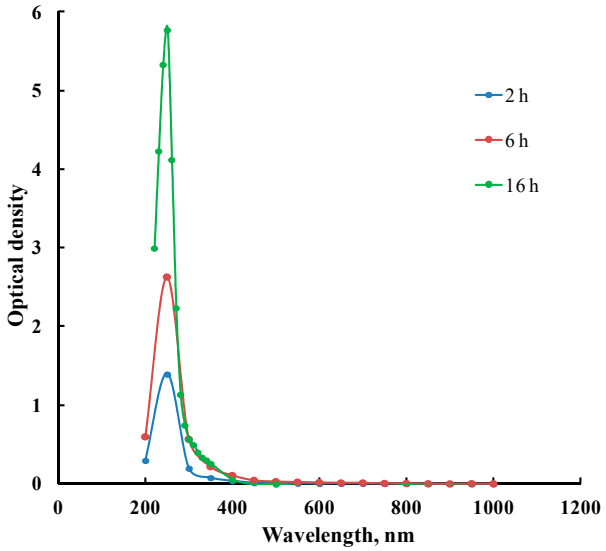

Figure 2. The polyethylene glycol (PEG) optical spectra after the thermal treatment at 120 °C with respect to the initial PEG.

To get insight into the degradation process, the samples of pure NMP and the mixture of NMP with PEG (75/25 wt%) were also annealed at the temperature of 120 °C. It should be pointed out that both spectra for untreated NMP and NMP/PEG samples were nearly the same and they are transparent in the visible range. However, the pronounced difference in their behavior was found during heat treatment as can be seen from the optical spectra in Figure 3. In both spectra of thermally treated samples, a shoulder appears with the maximal optical density in the blue-violet region of the spectrum, which decreases along the long-wave region of spectra. This explains the yellow-orange color of the thermally treated liquids since blue is an additional color to yellow and orange. It is known [46,47] that NMP has a tendency for oxidation in the presence of oxygen from the air at an elevated temperature with the formation of yellow-brown colored products of its oxidation and followed polymerization (gumming). The increase of optical density with the time of thermal treatment at 120 °C indicates the

accumulation of NMP degradation products. To get the insight of the degradation process, the samples of pure NMP and the mixture of NMP with PEG (75/25 wt%) were also annealed at the temperature of 120 °C. It should be pointed out that both spectra for untreated NMP and NMP/PEG samples were nearly the same and they are transparent in the visible range. However, the pronounced difference in their behavior was found during heat treatment as can be seen from the optical spectra Figure 3. In both spectra of thermally treated samples, a shoulder appears with the maximal optical density in the blue-violet region of the spectrum, which decreases along the long-wave region of spectra. This explains the yellow-orange color of the thermally treated liquids since blue is an additional color to yellow and orange. It is known [46,47] that NMP has a tendency for oxidation in the presence of oxygen from the air at an elevated temperature with the formation of yellow-brown colored products of its oxidation and followed polymerization (gumming). The increase of optical density with the time of thermal treatment at 120 °C indicates the accumulation of NMP degradation products.

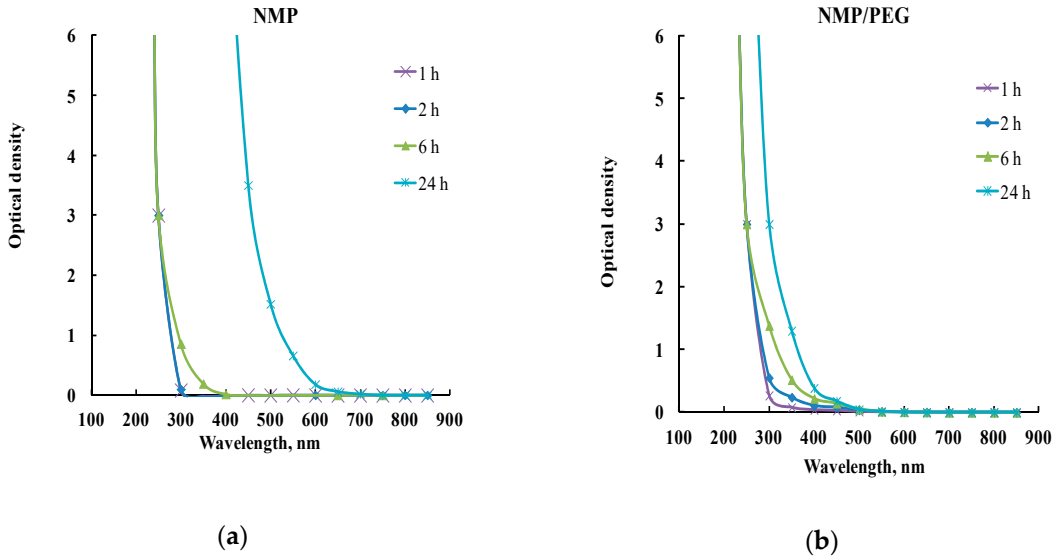

(**a**) (**b**)

Figure 3. The N-methyl-2-pyrrolidone (NMP) and NMP/PEG (75/25) optical spectra after the thermal treatment at 120 °C with respect to the initial NMP (**a**) and NMP/PEG (**b**).

In the first 1–6 h of thermal treatment, the intensity of NMP and NMP/PEG light absorption builds up slowly. However, after 24 h of thermal treatment, the intensity of coloration and optical density of NMP becomes markedly higher compared to the NMP/PEG mixture. It seems that the addition of PEG in NMP led to a less pronounced degradation process in contrast to pure NMP. Bearing in mind the fact that PEG molecules might also interact with the dissolved oxygen or other components presented in a common solution, the effect of hydroxyl groups on NMP degradation was evaluated. To this end, NMP solvent was also heated for 24 h at 120 °C in the presence of 5 wt% of ethylene glycol (EG) or 25 wt% tetraethylene glycol dimethyl ether (tetraglyme). Tetraglyme, being analog of PEG, does not contain ending hydroxyl groups since they are replaced with the dimethyl ether group; while ethylene glycol is a diol. It is interesting to notice from Figure 4 that both systems of pure NMP and NMP/tetraglyme did not reveal a noticeable difference in the optical spectra that might indicate a certain similarity in the degradation process; meanwhile, the presence of ethylene glycol and PEG allowed to reduce the coloration of the NMP-based solution. Thus, it allows to conclude that the hydroxy groups presented in PEG or ethylene glycol shall play a noticeable role in the process of thermo-oxidative degradation of the NMP solvent and spinning solution, respectively.

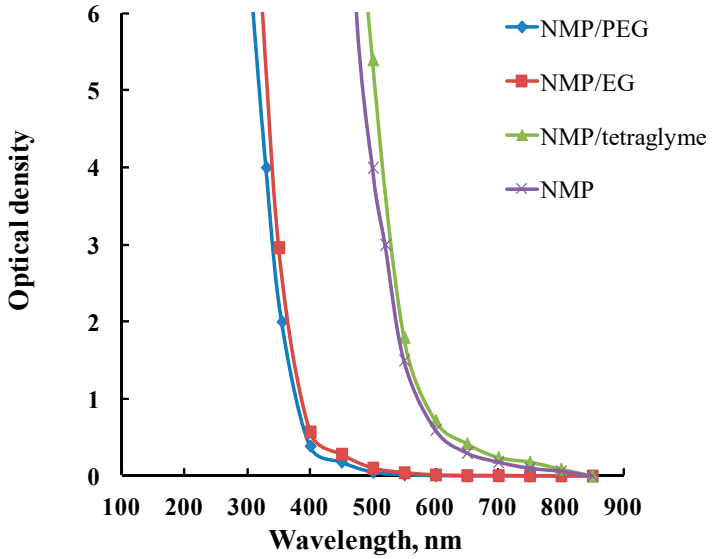

Figure 4. The optical spectra of NMP, NMP/PEG, NMP/ethylene glycol (EG), and NMP/tetraglyme after the thermal treatment at 120 °C for 24 h with respect to the initial samples.

The analysis of casting solutions is complicated due to their high viscosity and tendency to phase separation at the contact with water vapor from the air. Therefore, the same amount of each casting solution was coagulated in the fixed amount of water, then the coagulation bath was filtered through filter paper. The same procedure was also done for the reference spinning solution containing 23.9 wt% PSf in NMP without addition of PEG-400. It is important to notice that all filtered solutions were visually colorless, while the residuals, looked like resin and remained on filtered paper, had a light brown color, and were insoluble in water. The analysis of the optical density of the filtered coagulation bath used for precipitation of the PSf/NMP/PEG spinning solution revealed the peak at 270–280 nm, and the intensity of this peak was increased with a longer time of thermal exposure (see Figure 5). Furthermore, it can be noted that exposition time has more effect on the intensity of absorption than the treatment temperature because the higher peak was observed in the case of 16 h treatment at 120 °C compared with 11 h at 140 °C. Since no such a peak was found in the case of the reference PSf solution (without addition of PEG), it can be concluded that the water-soluble components of the degraded solution have PEG-based origin, and PEG reacts in the spinning solution at a high temperature.

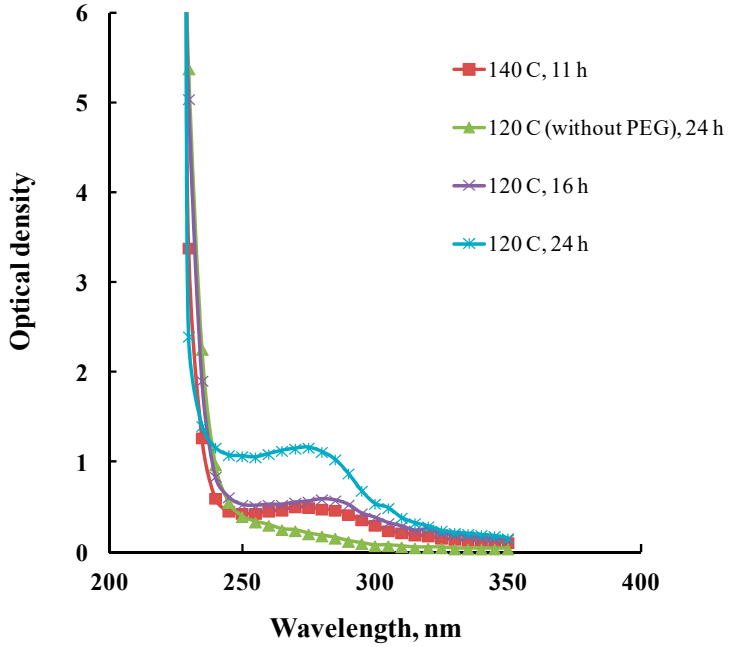

Figure 5. The optical spectra of the water phase after polysulfone (PSf) precipitation with respect to the water phase without PEG.

3.2. Flat Membranes

It is important to emphasize that the chemical interactions of the components of the casting solution during the heat treatment process have a significant effect on the viscosity of the solution resulted in a change of the membrane morphology and their transport characteristics. In the beginning, the effect of thermal treatment on the membrane characteristics was evaluated by using the flat-sheet configuration of membranes. As can be seen from Table 2, an increase in the heat treatment time from 6 to 24 h leads to an increase in the viscosity of the casting solution by a factor of 1.5. The structure of the membranes was visualized and examined using SEM (Figure 6). It was found that the membranes have an asymmetric structure with the thin selective layer and the porous support pierced with elongated macrovoids, and the flat-sheet membranes with a similar structure were obtained in studies [43,48]. The thickness of the fine-porous selective layer was estimated by analysis of SEM cross-sections and the obtained values are listed in Table 2. A substantial increase in the selective layer thickness from 3 to 15 μm was observed with the rise of the thermal treatment time, which might be attributed to the increase of the casting solution viscosity. However, the overall membrane thickness remains nearly the same, at around 100 μm. This is connected to the fact that the casting solution was applied on a glass plate using the casting blade with a 200 μm size of the gap, and the polymer concentration is supposed to be the same during the thermal treatment.

Table 2. Geometrical and gas transport characteristics of flat polysulfone (PSf) membranes.

Time of Treatment, h	Viscosity, cP	Membrane Thickness, μm	Selective Layer Thickness, μm	P/l (He), $m^3/(m^2 \cdot h \cdot atm)$	P/l (CO_2), $m^3/(m^2 \cdot h \cdot atm)$	α (He/CO_2)
6	31,200	102	3	41.1	15.9	2.6
11	37,000	103	10	22.2	7.9	2.8
16	39,900	99	11	19.3	6.6	3.0
24	46,900	102	15	8.7	2.9	3.0

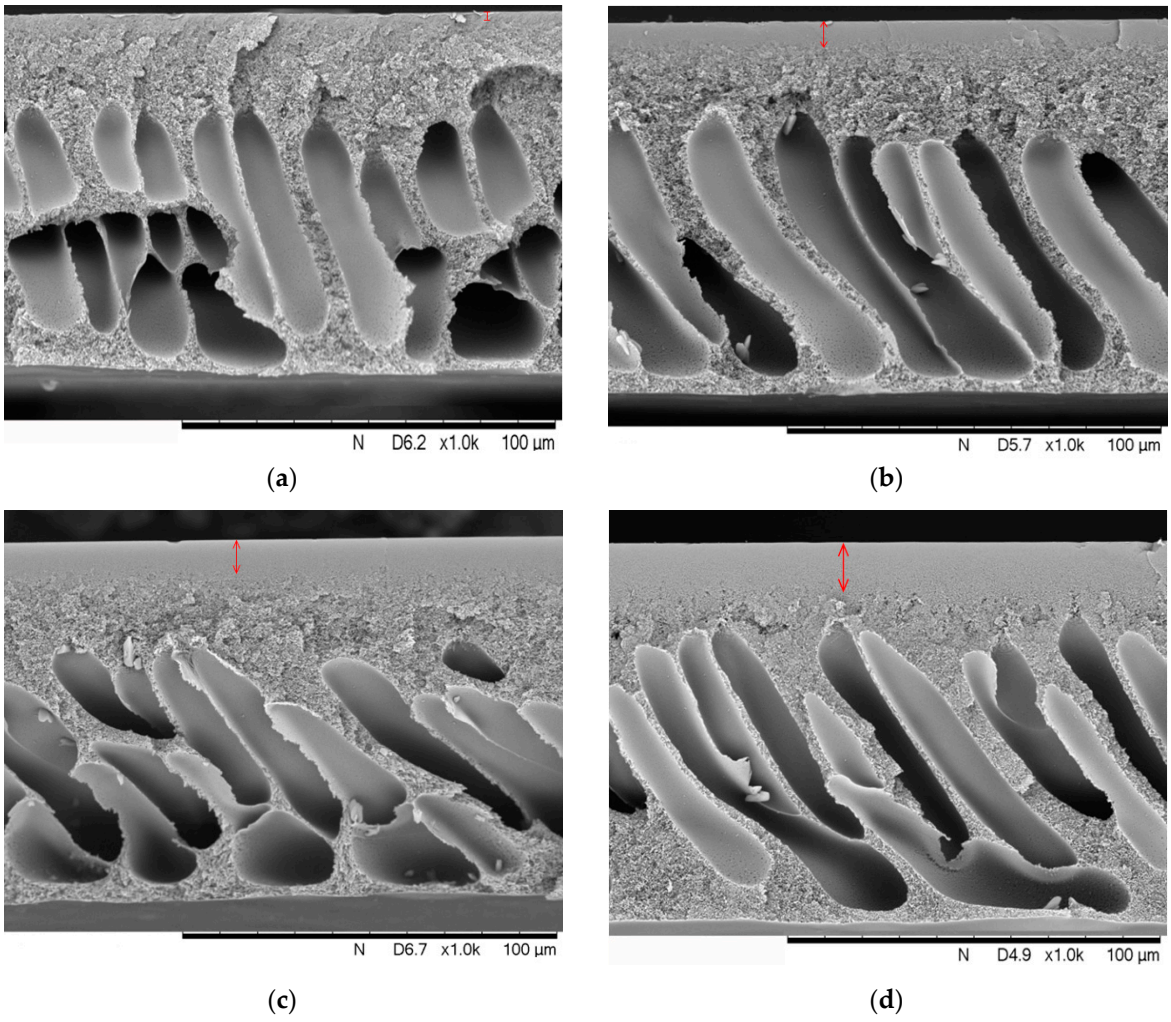

Figure 6. Scanning electron microscopy (SEM) micrographs of flat PSf membranes obtained from solutions with different time of thermal treatment at 120 °C (**a**) 6 h, (**b**) 11 h, (**c**) 16 h, (**d**) 24 h.

A change in the thickness of the selective layer naturally affects the transport properties of resulted membranes. For instance, a five time increase of the selective layer thickness from 3 to 15 µm resulted in about five times the decline of the gas permeance (see Table 2) since the fine-porous selective layer introduces the major contribution in the mass-transport resistance of the whole membrane. Sponge-like and macroporous layers act as support in the asymmetric membrane. The rise of the ideal selectivity α (He/CO_2) with the increase of the selective layer thickness is worth noting. The maximal ideal selectivity α (He/CO_2) = 3.0 is observed for the selective layer thickness of 15 µm. This value is close to the value of selectivity α (He/CO_2) = 3.3, which is typical for the Knudsen flow. Thus, it may be concluded that in the case of flat asymmetric membranes, the change in the chemical composition of low-molecular components of the casting solution and its viscosity during the thermal treatment leads to the increase of the selective layer thickness and its densification. Similar dependencies were observed in the work [49], where the effect of PSf concentration in the casting solution on the gas transport properties of flat-sheet membranes was studied. With the increase of polysulfone concentration, the casting solution viscosity increased, which, in turn, explained the decline of gas permeance and the rise of membrane selectivity.

3.3. Hollow Fiber Membranes

Figure 7 presents SEM images of the cross-section (up) and external surface (down) of hollow fiber membranes, obtained from the spinning solutions treated with a different time at 120 °C. Evidently, the membranes have an asymmetric structure with the thin selective layer and the porous support pierced with finger-like macrovoids. Meanwhile, for the first sample (6 h of thermal treatment), macropores revealed on the outer side of the hollow fiber membrane. The increase of thermal treatment time (11, 16, and 24 h) resulted in the formation of the sponge-like structure of the undersurface layer from the outer side of the membrane, and in the case of 24 h of treatment, the thickness of this layer was around 50 μm.

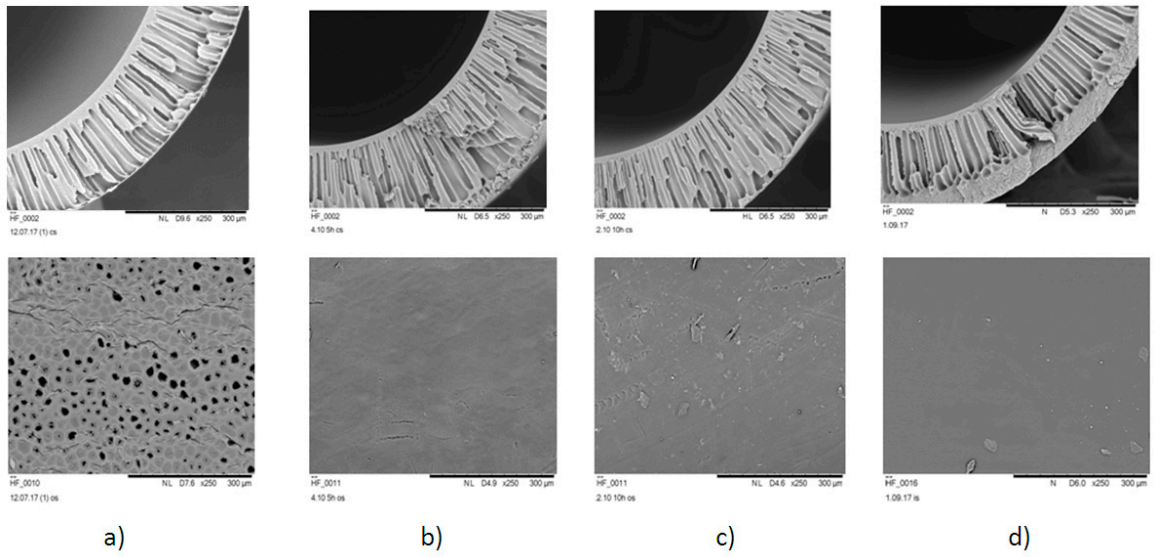

Figure 7. SEM images of the cross-sections (upper row) and the outer surface (lower row) of the hollow fiber membranes obtained from solutions with different time of thermal treatment at 120 °C: (**a**) 6 h, (**b**) 11 h, (**c**) 16 h, (**d**) 24 h.

By analysis of the SEM images, the geometrical parameters of the fiber, such as average outer and inner diameters (d_{out} и d_{in}) and fiber wall thickness were estimated. Besides, the average weight of 1 meter of fiber (m_l) was also determined. Given the outer and inner diameters of the fiber, and the weight of its unit length, the average density was calculated by using the following equation:

$$\rho = \frac{4m_l}{\pi\left(d_{out}^2 - d_{in}^2\right)},\ \mathrm{g/cm^3}\ . \tag{5}$$

The diameters d and average weight of fiber m_l were given in cm and g/cm, respectively.

It is well-known that the morphology and transport properties of the phase-inversion membranes substantially depend on the thermodynamic stability of casting solutions and the kinetics of the phase decay [16,50]. It can be seen from Table 3 that all membrane samples have close coagulation values. Therefore, despite the chemical transformations taking place in the casting solution, the stability of corresponded polymeric solutions towards the coagulation did not change. Consequently, the differences in the membrane morphology with the increase of thermal treatment time shall be connected with the coagulation kinetics.

Table 3. Properties of the casting solutions, density, and gas permeability of the hollow fiber membranes.

Treatment Time, h	Viscosity, cP	Coag. Value, g/g	Density, g/cm^3	P/l (He), m^3/(m^2·h·atm)	P/l (CO_2), m^3/(m^2·h·atm)	α (He/CO_2)
6	31,100	0.182	0.253	580	240	2.4
11	37,300	0.183	0.276	54	18	3.0
16	40,100	0.183	0.284	42	13	3.3
24	46,800	0.185	0.313	30	10	3.3

With increasing heat treatment time, the viscosity of the spinning solution increased significantly. The rate of phase separation is determined by the diffusion of the non-solvent (water) into the polymeric solution. With an increase in the viscosity of the solution, the diffusion flux of the non-solvent into the PSf solution decreases, and the relaxation time of polymer chains in the solution also increases [16,50]. This leads to a slowdown in phase decomposition and the formation of a denser membrane structure (increase in membrane density from 0.253 to 0.313 g/cm^3, Table 2) with less pronounced macropores (Figure 7).

In the case of flat-sheet membranes preparation, the solution was placed on the glass surface. Thereby, the coagulant (water) contacted with only one side of the membrane. However, the hollow fiber membranes were obtained in the free fall spinning mode, i.e., at the outlet of the casting solution from the spinneret, the inner surface was brought into contact with the internal coagulant (water). After passing the air gap, the fiber fell into the take-up bath with water. Thereby, from that moment, the outer surface of the membrane began to contact the coagulant.

The lowest solution viscosity (31,100 cP, 6 h) allows forming an asymmetric membrane structure through the whole wall thickness of the hollow fiber during the time of the air gap passage. Therefore, only in this case, macropores outcrop on the external surface of the hollow fiber (Figure 7). The increase of the solution viscosity results in the asymmetric membrane structure not having enough time to fully form along the whole thickness of the hollow fiber and at the outer surface of the membrane spongy structure is formed. For the solution with viscosity 46,800 cP (24 h), its thickness is around 50 μm (Figure 7).

The analysis of gas permeance and ideal He/CO_2 selectivity revealed that the increase of thermal treatment time and the solution viscosity resulted in the decline of gas permeance and an increase of selectivity. At the exposure time at 120 °C of 16 h or greater, He/CO_2 selectivity was equal to 3.3, which conforms to the Knudsen flow. The increase of selectivity indicates the decrease of the selective layer pore size due to its densification, while the decrease of gas permeance can be associated with the densification of the selective layer and the formation of the sponge-like layer at the outer side of hollow fibers at the time of 11 h or greater. Similar correlations were obtained in work [51], where the effect of spinning temperature on the structure and transport properties of ultrafiltration asymmetric hollow fiber membranes made of PSf was studied. With the increase of the temperature, the solution viscosity was reduced significantly, which resulted in the slowdown of the polymer coagulation process, a decrease of the dense selective membrane layer thickness, the rise of the water flux through the membrane and reduction of the nominal molecular weight cut-off in the process of dextrane water solution separation [51].

4. Conclusions

The thermal treatment of the casting solution substantially affects the morphology and transport properties of porous flat-sheet and hollow fiber membranes made of polysulfone. It was found that with increasing of exposure time at a temperature of 120 °C, the color intensity of the casting solution was increased. Spectrophotometric studies showed that the coloration appearance is associated with the NMP thermo-oxidative destruction with the formation of yellow-brown products. Meanwhile, hydroxyl groups of PEG actively react in the thermo-oxidative destruction of the casting solution.

The results obtained are relevant to any polymeric casting solution containing NMP and/or PEG and treated at temperatures above 60 °C.

It is found that the casting solution viscosity monotonically rises with the increase of the thermal treatment time. It was concluded that despite the chemical transitions occurring in the casting solutions, their stability towards coagulation does not virtually change. The difference in the membrane morphology with the growth of the thermal treatment time is associated not with the thermodynamic properties of the polymer solutions, but with the phase decay kinetics.

All obtained flat and hollow fiber membranes have an asymmetric structure with the selective layer and the porous support pierced with finger-like macrovoids. In the case of flat membranes, the rise of thermal treatment time leads to the growth of the selective layer thickness, which results in the decline of the gas permeance. Meanwhile, the increase of the ideal He/CO_2 selectivity allows concluding that the selective layer compacts with the rise of the thermal treatment time.

The hollow fiber selective layer was formed at the inner side of the membrane. Meantime, only for the hollow fiber sample, with 6 h of thermal treatment macrovoids outcrop on the external surface of the membrane. The increase of thermal treatment time (11, 16, and 24 h) leads to the formation of a sponge-like layer at the outermost surface of the membrane, therewith, in case of 24 h treatment, the thickness of this layer is around 50 μm. After more than 16 h of the solution thermal treatment, the He/CO_2 selectivity is equal to 3.3, which conforms to the Knudsen gas flow. The increase of selectivity suggests the decrease of the selective layer pore size due to densification. The decline of gas permeance with the rise of thermal treatment time is associated both with the selective layer densification and with the formation of a sponge-like layer at the outermost surface of the membrane.

Author Contributions: Conceptualization, I.B., A.V. and V.V. (Vladimir Volkov); methodology, V.V. (Vladimir Vasilevsky), I.B.; investigation, D.M., A.O.; data analysis, I.B., V.V. (Vladimir Vasilevsky), D.M., A.V. and V.V. (Vladimir Volkov); writing—original draft preparation, I.B.; writing—review and editing, V.V. (Vladimir Volkov), D.M. and A.V.; supervision, V.V. (Vladimir Volkov).

Funding: This work was carried out within the State Program of the A.V.Topchiev Institute of Petrochemical Synthesis, Russian Academy of Sciences (TIPS RAS).

Acknowledgments: The authors thank D.S. Bakhtin for SEM analysis, and Kirill Kutuzov for his assistance in experimental work.

Conflicts of Interest: The authors declare no conflict of interest.

References

1. Baker, R.W. *Membrane Technology and Applications*, 2nd ed.; John Wiley & Sons Ltd: Chichester, UK, 2004; pp. 191–354.
2. Mulder, J. *Basic Principles of Membrane Technology*; Kluwer Academic: Dordrecht, The Netherlands, 1996; pp. 51–58.
3. Ran, F. *Encyclopedia of Membranes*; Drioli, E., Giorno, L., Eds.; Springer: Berlin/Heidelberg, Germany, 2016; pp. 1598–1600.
4. Ida, S. *Encyclopedia of Polymeric Nanomaterials*; Kobayashi, S., Müllen, K., Eds.; Springer: Berlin/Heidelberg, Germany, 2014; pp. 1528–1534.
5. Hołda, A.K.; Vankelecom, I.F. Integrally skinned PSf-based SRNF-membranes prepared via phase inversion—Part A: Influence of high molecular weight additives. *J. Membr. Sci.* **2014**, *450*, 512–521. [CrossRef]
6. Hołda, A.K.; Vankelecom, I.F. Integrally skinned PSf-based SRNF-membranes prepared via phase inversion—Part B: Influence of low molecular weight additives. *J. Membr. Sci.* **2014**, *450*, 499–511. [CrossRef]
7. Ovcharova, A.; Vasilevsky, V.; Borisov, I.; Bazhenov, S.; Volkov, A.; Bildyukevich, A.; Volkov, V. Polysulfone porous hollow fiber membranes for ethylene-ethane separation in gas-liquid membrane contactor. *Sep. Purif. Technol.* **2017**, *183*, 162–172. [CrossRef]

8. Kostyanaya, M.; Bazhenov, S.; Borisov, I.; Plisko, T.; Vasilevsky, V. Surface Modified Polysulfone Hollow Fiber Membranes for Ethane/Ethylene Separation Using Gas-Liquid Membrane Contactors with Ionic Liquid-Based Absorbent. *Fibers* **2019**, *7*, 4. [CrossRef]
9. Marino, T.; Blasi, E.; Tornaghi, S.; Di Nicolò, E.; Figoli, A. Polyethersulfone membranes prepared with Rhodiasolv® Polarclean as water soluble green solvent. *J. Membr. Sci.* **2018**, *549*, 192–204. [CrossRef]
10. Dong, X.; Al-Jumaily, A.; Escobar, I. Investigation of the use of a bio-derived solvent for non-solvent-induced phase separation (NIPS) fabrication of polysulfone membranes. *Membranes* **2018**, *8*, 23. [CrossRef] [PubMed]
11. Wang, H.H.; Jung, J.T.; Kim, J.F.; Kim, S.; Drioli, E.; Lee, Y.M. A novel green solvent alternative for polymeric membrane preparation via nonsolvent-induced phase separation (NIPS). *J. Membr. Sci.* **2019**, *574*, 44–54. [CrossRef]
12. Marino, T.; Galiano, F.; Simone, S.; Figoli, A. DMSO EVOL™ as novel non-toxic solvent for polyethersulfone membrane preparation. *Environ. Sci. Pollut. Res.* **2018**, *26*, 14774–14785. [CrossRef] [PubMed]
13. Marino, T.; Galiano, F.; Molino, A.; Figoli, A. New frontiers in sustainable membrane preparation: Cyrene™ as green bioderived solvent. *J. Membr. Sci.* **2019**, *580*, 224–234. [CrossRef]
14. Kim, I.C.; Lee, K.H. Effect of various additives on pore size of polysulfone membrane by phase-inversion process. *J. Appl. Polym. Sci.* **2003**, *89*, 2562–2566. [CrossRef]
15. Chakrabarty, B.; Ghoshal, A.K.; Purkait, M.K. Effect of molecular weight of PEG on membrane morphology and transport properties. *J. Membr. Sci.* **2008**, *309*, 209–221. [CrossRef]
16. Kim, J.H.; Lee, K.H. Effect of PEG additive on membrane formation by phase inversion. *J. Membr. Sci.* **1998**, *138*, 153–163. [CrossRef]
17. Zheng, Q.Z.; Wang, P.; Yang, Y.N. Rheological and thermodynamic variation in polysulfone solution by PEG introduction and its effect on kinetics of membrane formation via phase-inversion process. *J. Membr. Sci.* **2006**, *279*, 230–237. [CrossRef]
18. Boom, R.M.; Van den Boomgaard, T.; Smolders, C.A. Mass transfer and thermodynamics during immersion precipitation for a two-polymer system: Evaluation with the system PES-PVP-NMP-water. *J. Membr. Sci.* **1994**, *90*, 231–249. [CrossRef]
19. Chakrabarty, B.; Ghoshal, A.K.; Purkait, M.K. Preparation, characterization and performance studies of polysulfone membranes using PVP as an additive. *J. Membr. Sci.* **2008**, *315*, 36–47. [CrossRef]
20. Miyano, T.; Matsuura, T.; Sourirajan, S. Effect of polyvinylpyrrolidone additive on the pore size and the pore size distribution of polyethersulfone (Victrex) membranes. *Chem. Eng. Commun.* **1993**, *119*, 23–39. [CrossRef]
21. Tsai, H.A.; Li, L.D.; Lee, K.R.; Wang, Y.C.; Li, C.L.; Huang, J.J.; Lai, Y. Effect of surfactant addition on the morphology and pervaporation performance of asymmetric polysulfone membranes. *J. Membr. Sci.* **2000**, *176*, 97–103. [CrossRef]
22. Fung-Ching, L.; Da-Ming, W.; Cheng-Lee, L.; Juin-Yih, L. Effect of surfactants on the structure of PMMA membranes. *J. Membr. Sci.* **1997**, *123*, 281–291. [CrossRef]
23. Mousavi, S.M.; Zadhoush, A. Investigation of the relation between viscoelastic properties of polysulfone solutions, phase inversion process and membrane morphology: The effect of solvent power. *J. Membr. Sci.* **2017**, *532*, 47–57. [CrossRef]
24. Reynolds, D.W.; Galvani, M.; Hicks, S.R.; Joshi, B.J.; Kennedy-Gabb, S.A.; Kleinman, M.H.; Parmar, P.Z. The use of N-methylpyrrolidone as a cosolvent and oxidant in pharmaceutical stress testing. *J. Pharm. Sci.* **2012**, *101*, 761–776. [CrossRef]
25. Glastrup, J. Degradation of polyethylene glycol. A study of the reaction mechanism in a model molecule: Tetraethylene glycol. *Polym. Degrad. Stabil.* **1996**, *52*, 217–222. [CrossRef]
26. Ray, W.J., Jr.; Puvathingal, J.M. A simple procedure for removing contaminating aldehydes and peroxides from aqueous solutions of polyethylene glycols and of nonionic detergents that are based on the polyoxyethylene linkage. *Anal. Biochem.* **1985**, *146*, 307–312. [CrossRef]
27. Han, S.; Kim, C.; Kwon, D. Thermal/oxidative degradation and stabilization of polyethylene glycol. *Polymer* **1997**, *38*, 317–323. [CrossRef]
28. Ismail, A.F.; Mansourizadeh, A. A comparative study on the structure and performance of porous polyvinylidene fluoride and polysulfone hollow fiber membranes for CO2 absorption. *J. Membr. Sci.* **2010**, *365*, 319–328. [CrossRef]

29. Idris, A.; Zain, N.M.; Noordin, M.Y. Synthesis, characterization and performance of asymmetric polyethersulfone (PES) ultrafiltration membranes with polyethylene glycol of different molecular weights as additives. *Desalination* **2007**, *207*, 324–339. [CrossRef]
30. Liu, F.; Xu, Y.Y.; Zhu, B.K.; Zhang, F.; Zhu, L.P. Preparation of hydrophilic and fouling resistant poly (vinylidene fluoride) hollow fiber membranes. *J. Membr. Sci.* **2009**, *345*, 331–339. [CrossRef]
31. Loh, C.H.; Wang, R.; Shi, L.; Fane, A.G. Fabrication of high performance polyethersulfone UF hollow fiber membranes using amphiphilic Pluronic block copolymers as pore-forming additives. *J. Membr. Sci.* **2011**, *380*, 114–123. [CrossRef]
32. Mansourizadeh, A.; Ismail, A.F.; Aroon, M.A. *Sustainable Membrane Technology for Energy, Water, and Environment*; Ismail, A.F., Matsuura, T., Eds.; John Wiley & Sons, Inc.: Hoboken, NJ, USA, 2009; pp. 191–201.
33. Ohya, H.; Shiki, S.; Kawakami, H. Fabrication study of polysulfone hollow-fiber microfiltration membranes: Optimal dope viscosity for nucleation and growth. *J. Membr. Sci.* **2009**, *326*, 293–302. [CrossRef]
34. Susanto, H.; Ulbricht, M. Characteristics, performance and stability of polyethersulfone ultrafiltration membranes prepared by phase separation method using different macromolecular additives. *J. Membr. Sci.* **2009**, *327*, 125–135. [CrossRef]
35. Wongchitphimon, S.; Wang, R.; Jiraratananon, R.; Shi, L.; Loh, C.H. Effect of polyethylene glycol (PEG) as an additive on the fabrication of polyvinylidene fluoride-co-hexafluropropylene (PVDF-HFP) asymmetric microporous hollow fiber membranes. *J. Membr. Sci.* **2011**, *369*, 329–338. [CrossRef]
36. Zhao, L.B.; Xu, Z.L.; Liu, M.; Wei, Y.M. Preparation and characterization of PSf hollow fiber membrane from PSf-HBPE-PEG400-NMP dope solution. *J. Membr. Sci.* **2014**, *454*, 184–192. [CrossRef]
37. Xu, Z.L.; Qusay, F.A. Effect of polyethylene glycol molecular weights and concentrations on polyethersulfone hollow fiber ultrafiltration membranes. *J. Appl. Polym. Sci.* **2004**, *91*, 3398–3407. [CrossRef]
38. Chen, H.Z.; Xiao, Y.C.; Chung, T.S. Multi-layer composite hollow fiber membranes derived from poly (ethylene glycol) (PEG) containing hybrid materials for CO2/N2 separation. *J. Membr. Sci.* **2011**, *381*, 211–220. [CrossRef]
39. Panda, S.R.; De, S. Preparation, characterization and performance of $ZnCl_2$ incorporated polysulfone (PSF)/polyethylene glycol (PEG) blend low pressure nanofiltration membranes. *Desalination* **2014**, *347*, 52–65. [CrossRef]
40. Moriya, A.; Maruyama, T.; Ohmukai, Y.; Sotani, T.; Matsuyama, H. Preparation of poly (lactic acid) hollow fiber membranes via phase separation methods. *J. Membr. Sci.* **2009**, *342*, 307–312. [CrossRef]
41. Prince, J.A.; Bhuvana, S.; Boodhoo, K.V.K.; Anbharasi, V.; Singh, G. Synthesis and characterization of PEG-Ag immobilized PES hollow fiber ultrafiltration membranes with long lasting antifouling properties. *J. Membr. Sci.* **2014**, *454*, 538–548. [CrossRef]
42. Bildyukevich, A.V.; Plisko, T.V.; Liubimova, A.S.; Volkov, V.V.; Usosky, V.V. Hydrophilization of polysulfone hollow fiber membranes via addition of polyvinylpyrrolidone to the bore fluid. *J. Membr. Sci.* **2007**, *524*, 537–549. [CrossRef]
43. Plisko, T.V.; Bildyukevich, A.V.; Karslyan, Y.A.; Ovcharova, A.A.; Volkov, V.V. Development of high flux ultrafiltration polyphenylsulfone membranes applying the systems with upper and lower critical solution temperatures: Effect of polyethylene glycol molecular weight and coagulation bath temperature. *J. Membr. Sci.* **2018**, *565*, 266–280. [CrossRef]
44. Yushkin, A.A.; Efimov, M.N.; Vasilev, A.A.; Ivanov, V.I.; Bogdanova, Y.G.; Dolzhikova, V.D.; Karpacheva, G.P.; Bondarenko, G.N.; Volkov, A.V. Effect of IR Radiation on the Properties of Polyacrylonitrile and Membranes on Its Basis. *Polym. Sci.* **2017**, *59*, 880–890. [CrossRef]
45. Bildyukevich, A.V.; Usosky, V.V. Prevention of the capillary contraction of polysulfone based hollow fiber membranes. *Pet. Chem.* **2014**, *54*, 652–658. [CrossRef]
46. Li, W.; Suelves, I.; Lazaro, M.J.; Zhang, S.F.; Morgan, T.J.; Herod, A.A.; Kandiyoti, R. Solvent degradation during coal liquefaction in a flowing-solvent reactor. *Fuel* **2004**, *83*, 157–179. [CrossRef]
47. Berrueco, C.; Alvarez, P.; Venditti, S.; Morgan, T.J.; Herod, A.A.; Millan, M.; Kandiyoti, R. Sample contamination with NMP-oxidation products and byproduct-free NMP removal from sample solutions. *Energy Fuels* **2009**, *23*, 3008–3015. [CrossRef]
48. Bildyukevich, A.V.; Plisko, T.V.; Isaichykova, Y.A.; Ovcharova, A.A. Preparation of high-flux ultrafiltration polyphenylsulfone membranes. *Pet. Chem.* **2018**, *58*, 747–759. [CrossRef]

49. Ismail, A.F.; Lai, P.Y. Effects of phase inversion and rheological factors on formation of defect-free and ultrathin-skinned asymmetric polysulfone membranes for gas separation. *Sep. Purif. Technol.* **2003**, *33*, 127–143. [CrossRef]
50. Smolders, C.A.; Reuvers, A.J.; Boom, R.M.; Wienk, I.M. Microstructures in phase-inversion membranes. Part 1. Formation of macrovoids. *J. Membr. Sci.* **1992**, *73*, 259–275. [CrossRef]
51. Dahe, G.J.; Teotia, R.S.; Bellare, J.R. Correlation between spinning temperature, membrane morphology, and performance of Psf/PVP/NMP/Water hollow fiber membrane forming system. *J. Appl. Polym. Sci.* **2012**, *124*, 134–146. [CrossRef]